Spike Communication of Dynamic Stimuli: Rate Decoding versus Temporal Decoding

David H. Goldberg and Andreas G. Andreou

Department of Electrical and Computer Engineering, Johns Hopkins University, 3400 N. Charles St., 105 Barton Hall, Baltimore, MD 21218 USA

Abstract

We compare two rudimentary methods for extracting information about a dynamic analog stimulus from a spike train: a rate decoder, which is based on the number of spikes in a counting window, and a temporal decoder, which is based on interspike intervals. We derive analytical models for the distortion between a stimulus current that drives an integrate-and-fire spike generator and a reconstruction of that current based on the spike train. We consider intrinsic distortion, which arises due to the limitations of spike coding, and extrinsic distortion, which is due to explicit alterations of the spike train. We find that in the absence of extrinsic distortion, the temporal decoder is superior to the rate decoder. In the presence of extrinsic distortion, the temporal decoder is preferred when low latency is required, but the rate decoder is preferred when the latency requirement is relaxed.

Keywords: Spike communication, rate coding, temporal coding, efficiency

1 Introduction

We compare two rudimentary methods for extracting information about a dynamic analog stimulus from a spike train: a rate decoder and a temporal decoder. The rate decoder is based on the number of spikes in a counting window, which is proportional to the "average rate". The temporal decoder is based on the precise temporal pattern of spikes, specifically the inverse of the interspike intervals, which is proportional to the "instantaneous rate". The decoders' performance is quantified by how well they reconstruct the current that drives an integrate-and-fire spike generator. We consider two distinct types of distortion: intrinsic distortion, which arises due to the limitations of spike coding; and extrinsic distortion, which is due to explicit alterations of the spike train, such as spike jitter or spike deletions.

We acknowledge that, for the most part, neurons do not attempt to reconstruct the somatic activity of their inputs. On the contrary, many rich forms of computation are implemented from one neuron to the next. However, because we are interested in isolating the properties of the spike decoders themselves, we believe this reconstruction paradigm is appropriate, as it provides an upper limit on the amount of information that is available for neuronal computation. We also acknowledge that the decoders we examine are not "optimal" in any sense. Rather, we see them as two extreme examples which elucidate the relationship between intrinsic distortion, extrinsic distortion, and reconstruction latency.

The performance of rate codes and temporal codes have been compared qualitatively [3,6] and quantitatively [4,1,5]. In those studies, the authors used measures based on the entropy of spike trains. While this approach elucidates the limitations of the spike trains themselves, its use assumes that the encoding and decoding of the signal is lossless. Here, we consider realistic band-limited signals and how encoding them in the form of spike trains degrades information transfer. Therefore, we consider the reconstruction distortion as an alternative to measures based on the entropy of the spike train. Gabbiani [2] applied a similar approach to the study of the rate decoder. He described the reconstruction as proportional to a linearly filtered and half-wave rectified version of the stimulus. In contrast, we explicitly consider the impulsive nature of the spike train.

2 Methods

We have employed a simple mathematical framework to analyze the performance of spike decoders (Fig. 1). This framework captures many elements of real neurons, yet is simple enough to provide analytical results. We quantify the performance of the decoding schemes by the determining the distortion between a stimulus current W and a reconstruction based on the spike train $\hat{W}$, which is expressed by $\varepsilon^2 = E[(W-\hat{W})^2]$.

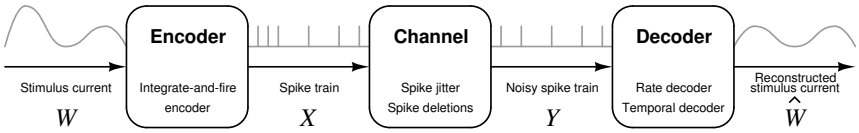

Fig. 1. Framework used to assess the performance of the spike decoding schemes.

Input To model the subthreshold activity in the soma, we use a stimulus current W that has a Gaussian amplitude distribution (mean μ_W and variance σ_W^2) and a low-pass frequency characteristic. The power spectral density and autocorrelation of W are given by

$$S_{WW}(\omega) = \frac{2\omega_c\sigma_W^2}{\omega_c^2+\omega^2} + 2\pi\mu_W^2\delta(\omega) \leftrightarrow R_{WW}(\tau) = \sigma_W^2 e^{-\omega_c|\tau|} + \mu_W^2 \tag{1}$$

where ω_c is the cut-off frequency (rad/sec).

Spike encoding Spike encoding in the axon hillock is represented by a non-leaky integrate-and-fire encoder which converts the input current into a spike train X. The current charges a capacitance C, and when the voltage on the capacitor V reaches the threshold θ, a spike is emitted and V is reset to zero. We can express the spike train X in terms of its ISIs $\{T_i^X\}$ and spike times $\{t_i^X\}$ as recursive function of W:

$$\theta = (1/C)\int_{t_{i-1}^X}^{t_{i-1}^X+T_i^X} w(t)dt \tag{2}$$

The spike train can be expressed as the sum of shifted delta functions, $x(t) = \sum_i \delta(t - t_i^X)$. The mean ISI μ_T and the mean spike rate λ can be expressed in terms of the integrate-and-fire parameters as $\mu_T = 1/\lambda = C\theta/\mu_W$.

Channel Axonal communication and synaptic transmission are represented by a channel that corrupts the spike train X by jittering and randomly deleting spikes, giving a noisy spike train Y. We model the spike jitter as a Gaussian random process that distorts the ISIs. If N is a Gaussian random variable where $N_i \sim \mathcal{N}(0, \sigma_T^2)$, then Y is given by $T_i^Y = T_i^X + N_i$. We model spike deletions by modulating the spike train with a Bernoulli process. If B be a Bernoulli random variable where $P(B_i = 1) = p$ and $P(B_i = 0) = 1 - p = q$, then Y is given by $y(t) = \sum_i B_i \delta(t - t_i^X)$.

Spike decoding The post-synaptic transformations at the efferent neuron are represented by the spike decoding process, which gives a reconstruction of the stimulus current $\hat{W}$. For the rate decoder, the reconstruction is given by

$$\hat{w}_{\text{rate}}(t) = C\theta\,[n(t,\tau)/\tau] \tag{3}$$

where $n(t,\tau)$ is the number of spikes in a sliding counting window given by $[t - \tau/2, t + \tau/2]$. The size of the counting window τ is a free parameter. For the temporal decoder, the reconstruction is proportional to the time between two spikes:

$$\hat{w}(t) = C\theta/T_i, \quad t_i < t < t_{i+1} \tag{4}$$

In all cases, the decoders are formulated such they are unbiased estimators of the input. The decoders, which are acausal as they have been defined, are made causal by assuming a latency between the stimulus at a particular instant and the reconstruction of the stimulus at that instant. In the case of the rate decoder, the latency is $\tau/2$, and in the case of the temporal decoder, the latency is the mean ISI $\mu_T/2$.

3 Distortion models

In this section, we give expressions for the distortion of the rate decoder and the temporal decoder. We consider two distinct types of distortion: intrinsic distortion, which arises due to the limitations of spike coding, and extrinsic distortion, which is due to explicit alterations of the spike train in the form of spike jitter and spike deletions. Because all of the noise sources we consider are independent, the distortion expressions can be summed to give the total distortion. All of the analytical models have been validated with simulations (not shown).

3.1 Rate decoder

Intrinsic distortion The spike counting window low-pass filters the stimulus current. This can be modeled by the convolution of the input signal $w(t)$ with a rectangular window

$h(t)$. The distortion is given by

$$\varepsilon^2_{\text{rate,lowpass}} = \int_{-\infty}^{\infty} S_{WW}(\omega) - 2S_{WW}(\omega)H^*(\omega) + H(\omega)S_{WW}(\omega)H^*(\omega)d\omega \tag{5}$$

The rate decoder has an additional intrinsic distortion source which arises from the discrete nature of spike counts, which we term quantization noise. This effect is not an artifact of the rectangular window—other low-pass filters display this behavior, although the quantization noise is replaced with a "ripple" that resembles the filter shape. Setting $n(t,\tau) = 1$ in Eq. 3 gives the quantization step $\Delta = C\theta/T_w$. It can be shown that the distortion arising from quantization noise is

$$\varepsilon^2_{\text{rate,quant}} = \Delta^2/6 \tag{6}$$

Fig. 2(a) shows a plot of the rate decoder intrinsic distortion as a function of window size τ. We see that increasing the window size has opposing effects on the two components of the intrinsic distortion: The quantization noise decreases because the quantization step is smaller, but the low-pass noise increases because the counting window smooths the input to a greater extent. This trade-off gives rise to an optimal window size that minimizes the intrinsic distortion.

Extrinsic distortion The effect of spike jitter on the rate code is subtle. Jitter causes a spikes near the edge of the counting window to be pushed into or out of the window. The distortion due to this effect, $\varepsilon^2_{\text{rate,jitter}}$, can be found by taking into account the Gaussian distribution of the spike jitter (expression not shown).

Spike deletions have a much more straightforward effect on the distortion. The number of spikes in a window that are preserved following deletion is given by the binomial distribution. The distortion due to spike deletion is given by

$$\varepsilon^2_{\text{rate,del}} = (\tau/\mu_T)(q/p)\Delta^2 \tag{7}$$

As shown in Fig. 2(b) and (c), the extrinsic distortion decreases with increasing window size. In general, this occurs because the larger window provides for more averaging and therefore increased robustness to variability in the spike train. Extrinsic distortion shifts the total distortion curve upward and to the right, increasing the optimal window size.

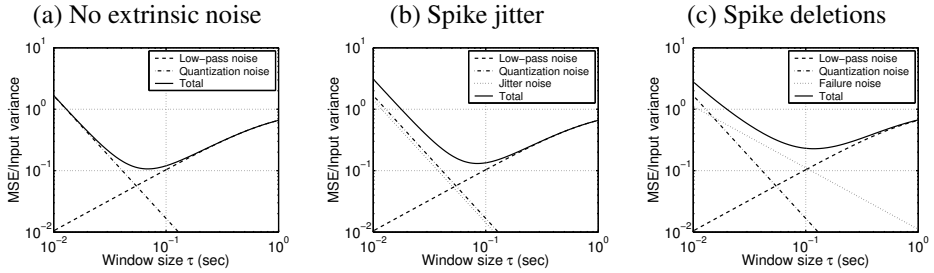

Fig. 2. Rate decoder distortion as a function of window size (parameters given in Appendix A). (a) No extrinsic noise. (b) Spike jitter, $\sigma_T/\mu_T = 20\%$. (c) Spike deletions, $q = 10\%$.

3.2 Temporal decoder

Intrinsic distortion The temporal decoder is also subject to low-pass effects, but the origin is the integrate-and-fire encoder, and the low-pass time constant is on the order of an ISI. If we assume that the spike train is regular i.e., σ_W/μ_W and σ_T/μ_T are small, then we can approximate the non-linear spike encoding and non-linear spike decoding as a convolution with a rectangular window with a width of μ_T (not shown).

Extrinsic distortion Spike jitter corrupts the ISIs, so its effect on the interval decoder is straightforward. The distortion can be found by a propagation of error approach:

$$\varepsilon^2_{\text{temp,jitter}} = \mu^2_{\hat{W}}\sigma^2_T/\mu^2_T \tag{8}$$

The deletion of spikes also introduces distortion for the temporal decoder. For example, the deletion of a single spike causes the two intervals delimited by the spike to be merged into a single interval, the length of which is given by the sum of the two original intervals. The general expression is given by

$$\varepsilon^2_{\text{temp,del}} = \sum_{y=1}^{\infty} y\left[\mu_W(1-(1/py))\right]^2 pP_Y(y) = \mu^2_W\left[(1/q)\ln(1/p)-1\right] \tag{9}$$

where $P_Y(y) = pq^{y-1}$ is the geometric density function, which describes the probability of having the first successful transmission on the yth trial.

4 Comparison

Now we are in a position to compare the rate decoder and the temporal decoder. The distortion models developed in the previous section enable us to freely explore the parameter space without the need for simulations. For the rate decoder, the size of the spike counting window τ is a free parameter. As discussed in Section 2, the window size of the rate decoder correspond is related to its latency. For the temporal decoder, the latency is related to the mean ISI.

In the absence of extrinsic distortion, the temporal decoder is preferred over the rate decoder at all window sizes (Fig. 3(a)). Extrinsic distortion causes both of the total distortion curves to be shifted upwards, but the rate decoder curve is shifted to a lesser extent (Fig. 3(b) and (c)). This occurs because the rate decoder is more robust to extrinsic noise by virtue of its abilities to average over many ISIs. Because the distortion curves cross in this case, we can partition the comparison into two regions. For low latencies, the temporal decoder is preferred, providing a "quick and dirty" estimate of the stimulus, whereas for high latencies, the rate decoder is preferred, providing a "slow and clean" estimate of the stimulus.

Fig. 4 compares the two decoders over a range of extrinsic distortion levels. We see that there is a distortion level for which the distortion curves never cross and the temporal decoder will always be preferred. As the distortion increases, the latency at which the curves cross decreases, albeit quite slowly.

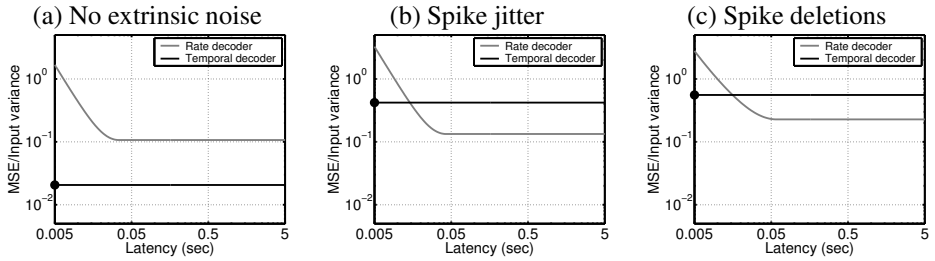

Fig. 3. Comparison of the rate decoder and the temporal decoder as a function of latency (parameters given in Appendix A). Rate decoder: The optimal distortion as a function of *maximum latency* (we plot the distortion at the latency at or below the point that gives the best performance). Temporal decoder: The dot is placed at the mean ISI. The solid line is drawn to facilitate comparison with the rate decoder. (a) No extrinsic noise. (b) Spike jitter, $\sigma_T/\mu_T = 20\%$. (c) Spike deletions, $q = 10\%$.

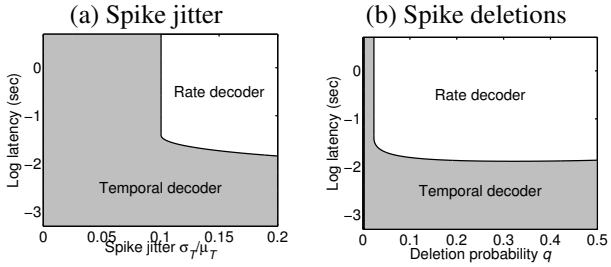

Fig. 4. Comparison of the rate decoder and the temporal decoder as a function of latency and extrinsic distortion (parameters given in Appendix A). In the gray region, the temporal decoder is preferred, and in the white region, the rate decoder is preferred.

5 Conclusion

The work presented here elucidates the intrinsic limitations of the spike decoding schemes and demonstrates how these schemes are influenced by physiological noise sources. The focus of future work is recast these decoders in terms of physiologically plausible mechanisms in order to make predictions about the nature of a spike coding for a given system on the basis of measurable physiological parameters. By constructing physical models of the decoders, we will also be able to determine how constraints such as power consumption influence the efficiency of spike coding.

A Nominal parameters

The parameters used to generate the figures are given below:

Symbol	Description	Value	Units
μ_W	Mean input current	1	μA
σ_W^2	Input current variance	0.1	μA^2
ω_c	Input current bandwidth	2π	rad/sec
λ	Mean spike rate	100	Hz
μ_T	Mean ISI	$1/\lambda$	sec
C	Membrane capacitance	1	μF
θ	Spike threshold	$\mu_I/(\lambda C)$	V

References

[1] R. Eckhorn, O. J. Grüsser, J. Kröller, K. Pellnitz, and B. Pöpel. Efficiency of different neuronal codes: Information transfer calculations for three different neuronal systems. *Biological Cybernetics*, 20:49–60, 1976.

[2] Fabrizio Gabbiani. Coding of time-varying signals in spike trains of linear and half-wave rectifying neurons. *Network: Computation in Neural Systems*, 7:61–85, 1996.

[3] Donald M. MacKay and Warren S. McCulloch. The limiting information capacity of a neuronal link. *Bulletin of Mathematical Biophysics*, 14:127–135, 1952.

[4] Anatol Rapoport and William J. Horvath. The theoretical channel capacity of a single neuron as determined by various coding schemes. *Information and Control*, 3:335–350, 1960.

[5] William R. Softky. Fine analog coding minimizes information transmission. *Neural Networks*, 9:15–24, 1996.

[6] Richard B. Stein. The information capacity of nerve cells using a frequency code. *Biophysical Journal*, 7:797–826, 1967.